tvst

DOI: 10.1167/tvst.4.6.6

Article

Feasibility of Structural and Functional MRI Acquisition with Unpowered Implants in Argus II Retinal Prosthesis Patients: A Case Study

Samantha I. Cunningham[1], Yonggang Shi[2], James D. Weiland[3], Paulo Falabella[3,4], Lisa C. Olmos de Koo[3], David N. Zacks[5], and Bosco S. Tjan[6,7]

[1] Department of Biomedical Engineering, University of Southern California, Los Angeles, CA, USA
[2] Laboratory of Neuro Imaging, USC Stevens Neuroimaging and Informatics Institute, Keck School of Medicine, University of Southern California, Los Angeles, CA, USA
[3] USC Eye Institute, University of Southern California, Los Angeles, CA, USA
[4] Department of Ophthalmology and Visual Sciences, Federal University of São Paulo, São Paulo, Brazil
[5] Kellogg Eye Center, University of Michigan, Ann Arbor, MI, USA
[6] Neuroscience Graduate Program, University of Southern California, Los Angeles, CA, USA
[7] Department of Psychology, University of Southern California, Los Angeles, CA, USA

Correspondence: Bosco S. Tjan, Department of Psychology, University of Southern California, SGM 501, 3620 McClintock, Los Angeles, CA 90089, USA. e-mail: btjan@usc.edu

Received: 3 June 2015
Accepted: 27 September 2015
Published: 8 December 2015

Keywords: retinal prothesis; retinitis pigmentosa; MRI; fMRI; dMRI

Citation: Cunningham SI, Shi Y, Weiland JD, et al. Feasibility of structural and functional MRI acquisition with unpowered implants in Argus II retinal prosthesis patients: a case study. Trans Vis Sci Tech. 2015; 4(6):6, doi:10.1167/tvst.4.6.6

Purpose: Magnetic resonance imaging (MRI) can measure the effects of vision loss and recovery on brain function and structure. In this case study, we sought to determine the feasibility of acquiring anatomical and functional MRI data in recipients of the Argus II epiretinal prosthesis system.

Methods: Following successful implantation with the Argus II device, two retinitis pigmentosa (RP) patients completed MRI scans with their implant unpowered to measure primary visual cortex (V1) functional responses to a tactile task, whole-brain morphometry, V1 cortical thickness, and diffusion properties of the optic tract and optic radiation. Measurements in the subjects with the Argus II implant were compared to measurements obtained previously from RP patients and sighted individuals.

Results: The presence of the Argus II implant resulted in artifacts that were localized around the patient's implanted eye and did not extend into cortical regions or white matter tracts associated with the visual system. Structural data on V1 cortical thickness and the retinofugal tract obtained from the two Argus II subjects fell within the ranges of sighted and RP groups. When compared to the RP and sighted subjects, Argus II patients' tactile-evoked cross-modal functional MRI (fMRI) blood oxygen level-dependent (BOLD) responses in V1 also fell within the range of either sighted or RP groups, apparently depending on time since implantation.

Conclusions: This study demonstrates that successful acquisition and quantification of structural and functional MR images are feasible in the presence of the inactive implant and provides preliminary information on functional changes in the brain that may follow sight restoration treatments.

Transitional Relevance: Successful MRI and fMRI acquisition in Argus II recipients demonstrates feasibility of using MRI to study the effect of retinal prosthesis use on brain structure and function.

Introduction

Structural and functional magnetic resonance imaging (MRI) has provided valuable information on the impact of blindness on central visual pathways. Numerous studies document the effects of vision loss on structural connectivity, but are limited in describing changes following treatment. A diffusion tensor imaging (DTI) study conducted with late-blind glaucoma patients found decreased diffusivity along the optic radiation.[1] However, other studies have demonstrated that structural connectivity changes are

minor or absent in individuals who lose their sight later in life: Li et al.[2] found that age at onset of blindness is correlated negatively with the mean number of connections throughout the cortex, with late-blind patients having a greater connectivity density (similar to that of sighted individuals) than early or congenitally blind patients. Other findings have demonstrated that late-blind retinitis pigmentosa (RP) subjects exhibit changes in cortical thickness, compared to their sighted counterparts, that are correlated with years since onset of blindness.[3] Understanding the effects of vision loss and recovery on white matter integrity and gray matter thickness not only provides insight into structural plasticity, but may help us predict how an individual will respond to treatment. In the case of electronic retinal prostheses,[4,5] compromised visual pathways could adversely affect treatment outcome.

Neuroimaging studies have also described the effects of vision recovery on cortical function following various types of restorative procedures. Vision restoration training in patients with 6 months to 8 years of cerebral blindness (resulting from postchiasmatic damage to the visual pathways) resulted in enlarged visual fields, while functional MRI (fMRI) further revealed a change in size and position of population receptive fields that accounted for local increases in visual field.[6] The cortical effects of sight restoration following long-term vision deprivation were documented extensively in a single individual by Fine et al.[7] After becoming bilaterally blind at the age of 3 years, subject MM only experienced minimal light perception until the age of 43 years, when he received a corneal and limbal stem-cell transplant in his right eye. Functional MRI responses following the surgery revealed that, while MM's fusiform gyrus and lingual gyrus showed little-to-no blood oxygen level-dependent (BOLD) responses to complex faces and objects, he exhibited normal responses in middle temporal (MT) and medial superior temporal (MST) areas to the motion of simple objects. In addition to these cases, cross-modal responses in the primary visual cortex (V1) have been proposed as a possible biomarker to investigate the effect of vision deprivation and restoration on the visual system. Cunningham et al.[10] found a significant correlation between vision loss and tactile-evoked activity in V1, where reduced visual acuity and visual field were associated with stronger and more extensive cross-modal responses. A similar pattern of tactile-evoked V1 activation was observed in sighted individuals after being blindfolded for 5 days and was reversed within 24 hours of removing the blindfold.[22] These studies use neuroimaging to explain psychophysical findings and provide evidence that the visual cortex of blind patients once again can process visual input following vision restoration, with the caveat that visual experience into adulthood is linked to the degree of vision recovery.[7]

Measurement of structural and functional changes in the brains of retinal prosthesis patients necessitates the acquisition of MR images that are free of excessive artifacts and noise. The Argus II epiretinal prosthesis (Second Sight Medical Products, Inc., Sylmar, CA)[4] is a treatment option for RP patients that consists of a small glasses-mounted video camera that captures and transmits video to a video processing unit (VPU). This VPU then converts the image into electrical signals that are conveyed to an external transmitter coil and wirelessly transmitted to a 6×10 microelectrode array that is implanted onto the surface of the retina.We sought to demonstrate the feasibility of acquiring high-quality MRI and fMRI data in Argus II patients with an inactive (unpowered) implant while in the MRI scanner. This included assessing how the presence of the inactive device affects V1 volumetric data, diffusion imaging of the optic tract and optic radiation, and normality of cross-modal tactile-evoked fMRI BOLD responses in V1. This will serve as a first step towards using MRI to study the short and long-term effects of retinal prosthesis use on cortical structure and function, as well as their association with patients' visual performance following treatment.

Materials and Methods

Participants

Two female subjects (ages 55 and 79 years old) participated in the study (Table 1). The Argus II retinal prosthesis was implanted successfully 6 weeks before our study in subject A1 and 15 weeks before our study in subject A2. In accordance with inclusion and exclusion requirements to receive the device,[8] both individuals had been diagnosed with RP and had a visual acuity of 2.3 logMAR or worse at implantation. Subjects were screened by their ophthalmologists before recruitment and had been advised previously to use their device for 2 to 6 hours per day following surgery.

The Argus II implant is labeled as MRI conditional, per Weiland et al.[9] The external components, camera, and VPU are not MRI safe and, therefore,

Table 1. Argus II Subject Demographics

Subject ID	Age, Sex	Visual Acuity	Date of Implantation	Implanted Eye	Can Subject Read Braille?	Diagnosis	Average Device Usage (Total Time with Device)
A1	55, F	<2.3 logMAR	June 2014	Left	No	RP	2–5 h/d (6 wks)
A2	79, F	<2.3 logMAR	February 2014	Right	No	RP	5–6 h/d (15 wks)

were removed before the subject entered the scanner room. We collected T1-weighted (T1w) structural images, diffusion MRI (dMRI) data, and task-state fMRI data from the two Argus II subjects. The fMRI data set from the Argus II subjects were compared to data from a group of 9 late-blind patients with RP and 9 sighted control subjects, previously described by Cunningham et al.[10] These 18 subjects had a mean ± SD age of 45.11 ± 13.78 years (range, 21–67 years); sighted control subjects were sex-matched and had a similar age range (24–66 years), as did the RP subjects (21–67 years, Supplemental Table S1). The RP group was divided into "Low Vision" ($n = 5$) and "Blind" ($n = 4$) subgroups. Those in the "Blind" subgroup had a visual acuity worse than 20/200 (logMAR = 1), a definition of legally blind. All remaining RP subjects were placed in the "Low Vision" subgroup.

The dMRI data from the Argus II subjects were compared to data obtained from the RP subjects. In addition, dMRI data from 14 healthy subjects randomly selected from the Human Connectome Project (HCP) Lifespan Pilot Phase 1a data set (age range, 25–78 years, Supplemental Table S2) were used as normal controls (dMRI data were collected from only 2 of the 9 sighted control subjects who participated in the study by Cunningham et al.[10] and, therefore, were insufficient). The study received approval from the University of Southern California's Health Sciences Campus Institutional Review Board, and all subjects provided written informed consent after explanation of the nature and possible consequences of the study. MRI experiments were conducted at the USC David and Dana Dornsife Cognitive Neuroscience Imaging Center, and indirect ophthalmic exams (in which the posterior segment of the eye was viewed using a hand-held lens and bright light) were conducted by an ophthalmologist from the USC Eye Institute during each MRI session. Subjects received monetary compensation for their participation. This research followed the tenets of the Declaration of Helsinki.

Image Acquisition

Magnetic resonance images for Argus II and RP subjects were acquired in a 3 Tesla Siemens (Munich, Germany) MAGNETOM TIM Trio scanner using a 12-channel Matrix head coil. For Argus II subjects, postoperative anatomical images were obtained using an MP-RAGE T1w sequence with TR/TE/TI/flip angle/slice thickness = 2.30 s/2.98 ms/900 ms/9°/1.2 mm.

Functional images with BOLD contrast for the tactile and visual tasks were acquired using an echo planar imaging (EPI) sequence with TR/TE/flip angle = 2 s/25 ms/60° and 3D PACE (Prospective Acquisition Correction). A total of 36 slices with isotropic voxels of 3 × 3 × 3 mm^3 were oriented axially and covered the entire cerebral cortex except for the tip of the temporal lobe for some subjects. The dMRI data were acquired for both Argus II subjects and 7 of the 9 RP subjects using a diffusion-weighted (DWI) imaging sequence (TR/TE = 10 s/88 ms), which included 60, 2-mm thick slices with isotropic voxels of 2 × 2 × 2 mm^3. A whole-brain dMRI protocol with 30 diffusion directions at a b-value of 900 s/mm^2 was repeated 3 times, each for a duration of 5:40 minutes.

Control subjects from the HCP LifeSpan Pilot Project Phase 1a underwent T1w MP-RAGE structural scans (TR/TE/TI/flip angle = 2.4 s/2.12 ms/1000 ms/8°) and DWI scans (TR/TE/flip angle = 3.67 s/74.8 ms/78°, 1.5 mm isotropic voxels) in a Siemens 3T Connectom Skyra. DWI data were acquired through 4 runs representing 2 different shells of b = 1000 and 2500 s/mm^2. Across these runs, there were 75 gradient directions in each shell. The data were downloaded from the ConnectomeDB (available in the public domain at https://db.humanconnectome.org).

Experimental Stimuli and Tasks

Both Argus II subjects completed the same three tactile tasks as the RP and sighted subjects from a

previous study,[10] in the following order: (1) a shapes task requiring subjects to determine if any of a series of raised-line shapes was bilaterally symmetric, (2) a Braille-dot counting task in which subjects counted the number of dots in a series of random Braille letters (subjects were not asked to read the letters), and (3) a sandpaper task requiring individuals to determine the relative roughness between a strip of sandpaper and the sandpaper disc surrounding it. Each subject was given a sheet composed of 4 columns and 5 rows of tactile elements spaced approximately 25 mm apart, for a total of 20 tactile elements per sheet. Subjects completed two sheets for each task using their dominant hand, where the second sheet consisted of the same tactile elements as the first in a rearranged order.

The tasks were performed in a block design paradigm, in which subjects scanned a column during active blocks and rested their fingers in the empty space between columns during rest blocks. Each run was composed of four 20-second active blocks (one active block per column) and five 20-second rest blocks. These blocks were interleaved, with the run starting and ending on a rest block. Subjects were given 4 seconds per tactile element (for a total of 20 seconds per active block/column) for determining symmetry, number of dots, or relative roughness and were instructed to either explore the tactile elements or rest between columns.

Subjects wore headphones, and auditory instructions were given under computer control using a text-to-speech function. These instructions also indicated when subjects should move from one tactile element to another in a column; the auditory instructions were presented during rest and active blocks. Participants did not report their answers during scanning. All subjects were asked to keep their eyes open while wearing a light-excluding eye mask (made of black molded cell foam and nylon interlock fabric with a contoured rim) throughout the task. The scanner and scanner room lights were turned off. All completed a training session before entering the scanner and completed a verbal survey about their performance following the scans to ensure that the task was completed properly.

Both Argus II subjects also completed a visual task in which a flickering checkerboard was presented during scanning. The subject was instructed to gaze directly upwards towards a clip-on mirror that was placed on the head coil in front of the subject's eyes. This mirror was oriented towards a rear-projection screen at the back of the scanner, allowing the subject to view the stimulus presentation. The screen size using the clip-on mirror was $23.6° \times 18.4°$ with a viewing distance of 85 cm. Two alternating black and white checkerboards (interleaved with a blank black screen) were flickered every 0.1 s. The stimulus was presented in a design blocked, in which the checkerboard flickered continuously during active blocks and a black screen was presented during rest blocks. Each run was composed of four 20-second active blocks and five 20-second rest blocks. These blocks were interleaved, with the run starting and ending on a rest block. This stimulus allowed us to determine the responsiveness of each subject's visual cortex to visual input.

Experimental Procedure

Both Argus II subjects completed two postoperative sessions after receiving the device. The device currently has Food and Drug Administration (FDA) approved labeling allowing for its conditional use in a 3T MRI, which specifies that under the conditions on the label, a person with an Argus II can enter an MRI scanner. As an added safety measure, a procedure was used that gradually added complexity to ensure the subject's device and implanted eye were unaffected by each set of scans (all scanning parameters complied with those specified in the FDA's approved MRI labeling for the device). Before entering the MRI machine, an ophthalmologist completed a baseline ophthalmic exam during which he examined the externally observable parts of the implanted eye and used an indirect ophthalmoscope to evaluate the retina and the prosthesis inside the eye after pupil dilation. A baseline device test then was conducted according to standard device assessment protocols designed by the Argus II manufacturer.

After verifying that the subject's implanted eye was stable in comparison with previous follow-up examinations and that the Argus II device was functioning properly, the subject entered the MRI scanner for 5 minutes without the external system—no scanning was completed at this time. After exiting the scanner room, a second ophthalmic exam and device functionality test were performed. A brief interview was conducted to determine if the subject felt any unusual sensations around her implanted eye while in the scanner room or scanner bore, including pressure, pain, phosphenes (spots of light), or heat. The subject then reentered the scanner without her external prosthesis coil and completed a series of anatomical scans, functional scans (including tactile

Table 2. Summary of Both Postoperative Scanning Procedures

	MRI Session #1	MRI Session #2
Before the session	■ IOE and baseline DFT outside of scanner	■ IOE outside of scanner
Part 1	■ Subject enters scanner for 5 minutes (no scanning) ■ IOE, DFT, and SI outside of scanner	■ Anatomical scanning ■ Series of tactile task functional scans ■ IOE, DFT, and SI outside of scanner
Part 2	■ Anatomical scanning ■ IOE, DFT, and SI outside of scanner	■ Anatomical scanning ■ Resting-state scan ■ Checkerboard functional scans ■ DWI scans ■ IOE, DFT, and SI outside of scanner
Part 3	■ Series of tactile task functional scans ■ IOE, DFT, and SI outside of scanner	
Part 4	■ Anatomical scanning ■ Resting-state scan ■ Checkerboard functional scans ■ DWI scans ■ IOE, DFT, and SI outside of scanner	

IOE, indirect ophthalmic exam; DFT, device functionality test; SI, subject interview.

and visual stimulus tasks), and DWI scans. The same indirect ophthalmoscopic exam, device functionality test, and subject interview were repeated following the anatomical scans, tactile tasks, and after the scanning session was complete (Table 2).

Functional MRI Data Analysis

Functional data analysis followed closely the procedures described by Cunningham et al.[10] Data were analyzed using BrainVoyager QX[11] in subjects' native space (as opposed to normalizing to a standard space). T1w anatomical data underwent inhomogeneity correction and were reoriented via rigid-body rotation and translation to place the origin at the anterior commissure, and the posterior commissure on the *y*-axis. Since both Argus II patients underwent multiple scanning sessions, anatomical scans from each were coregistered to each subject's first-session high resolution T1w data. All functional data were preprocessed with 3D motion correction, slice timing correction, and temporal filtering. In cases of excessive head movement, which occurred in subject A2, volumes in which a subject exhibited movement greater than 0.6 mm or 0.6 radians of motion and the corresponding entries in the design matrix were excluded from the analysis (a total of 16 seconds [<4.0%] of the data were removed from A2). Spatial smoothing was not applied to the functional data.

Whole-brain voxel-wise BOLD modulation was obtained by estimating the signal level during the active blocks with respect to that during the resting blocks using a general linear model (GLM), with head-motion parameters as covariates. For each subject, individual functional data sets of each run were concatenated after normalization (z-transform). Significant voxel-wise activations were identified at FDR < 0.05 with a minimum cluster size of 25 mm^2. Activation maps for each subject were constructed by projecting the GLM contrast (*t*-statistics) obtained from voxels on the cortex onto the reconstructed and inflated cortical surface meshes of the subject.

For the functional analysis, V1 and the primary somatosensory cortex (S1) were identified anatomically for each subject, with V1 consisting of both banks of the calcarine fissure, the parietal-occipital fissure, and the posterior end of the calcarine sulcus.[12] S1 extended from the middle of the central sulcus to the peak of the postcentral gyrus, and from the medial longitudinal fissure to the lateral sulcus. We calculated, for each subject, two complimentary measures (extent and strength) of the unsigned cross-modal response. The areal extent of cross-modal activation in V1 was defined as the percentage of significantly modulated voxels on the cortex within the V1 region of interest (ROI), while the strength of the response was calculated as the mean absolute parameter

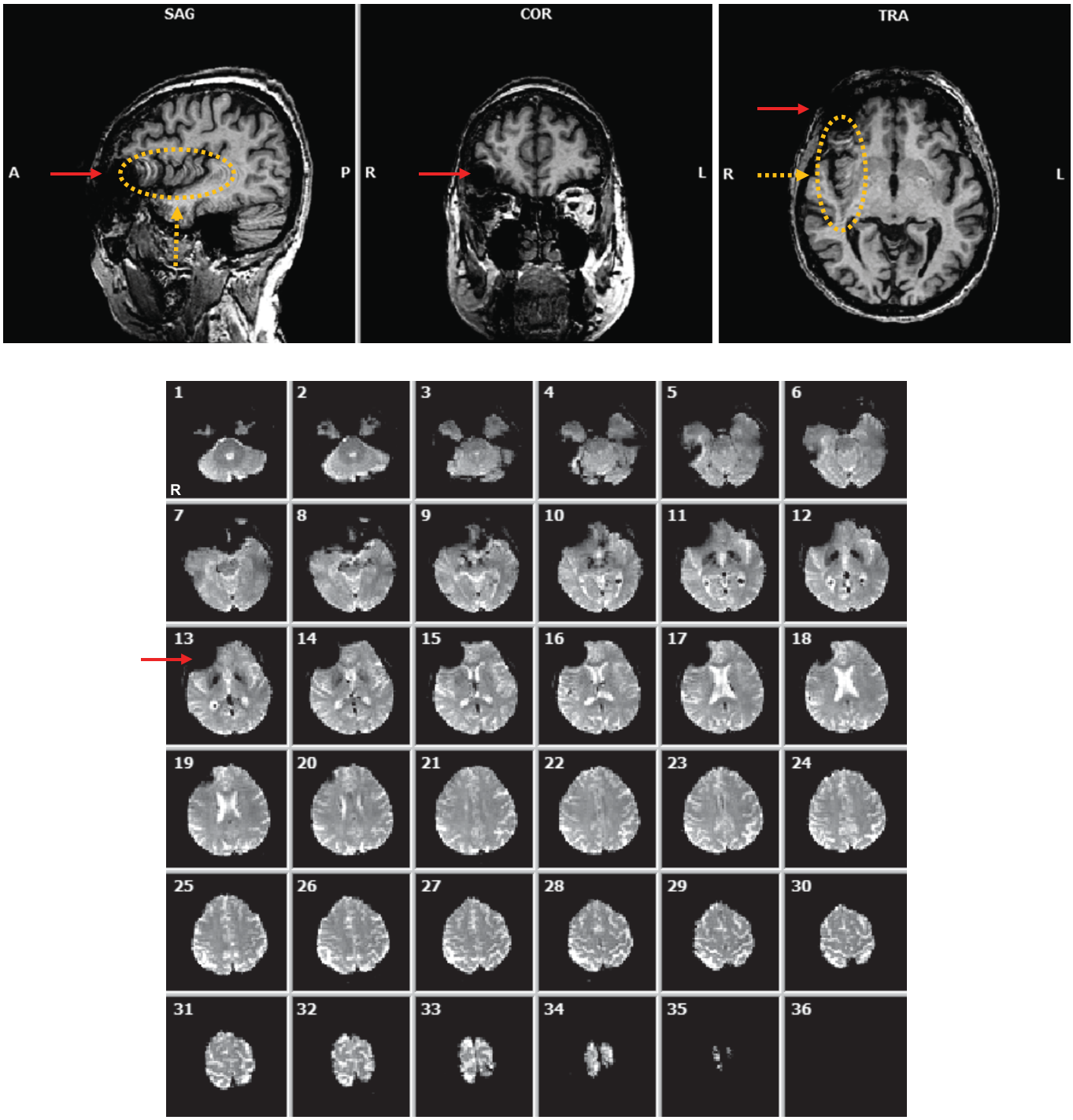

Figure 1. *Top*: Anatomical (MP-RAGE) image of subject A2 displaying local and nonlocal forms of artifact. *Bottom*: 36 functional (EPI) image slices showing presence of an artifact near the right eye (left side of images). *Red solid arrows*: local artifact resulting from the presence of the device implanted in the subject's right eye. *Orange dashed arrows* and *ellipse*: nonlocal artifact in the right hemisphere extended along the phase encoding direction (AP).

estimate (β value) of the responding voxels within the V1 ROI. The percentage of modulated voxels and mean absolute beta value of those voxels were similarly calculated within the S1 ROI. We then determined if the Argus II subjects fell within or outside of the ranges of either RP (blind or low vision) or sighted subjects based on descriptive statistics.

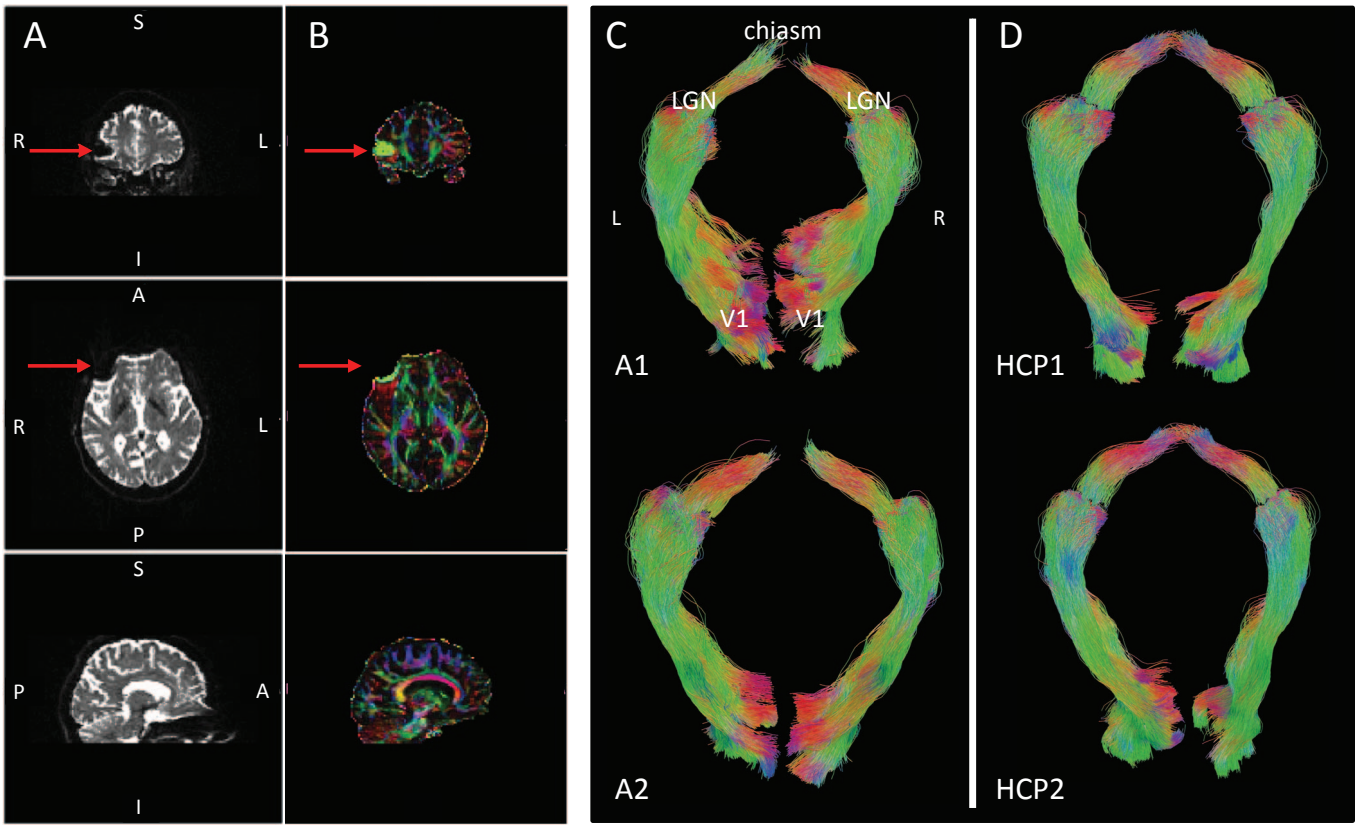

Figure 2. Diffusion results in Argus II and healthy control subjects. (**A**) Images ($b = 0$) of subject A2 obtained during DWI displaying artifact around the right implanted eye (following eddy correction of the data). (**B**) Fractional anisotropy (FA) computed from subject A2's DWI data overlaid with color-coded principal diffusion tensor directions. *Red arrows* indicate location of the local artifact resulting from the presence of the device implanted in the subject's right eye. (**C**) Automatically reconstructed retinofugal tract from optic chiasm to V1 based on the DWI data obtained from the two Argus II subjects using our custom procedure (see Materials and Methods). (**D**) Similarly reconstructed retinofugal tract in two representative HCP control subjects for comparison. Right brain hemisphere is on the side of the image indicated by "R."

Structural Data Analysis

T1w MP-RAGE images from all subjects were analyzed using FreeSurfer[13] to compute the white matter and pial surfaces.[13,14] Using these surfaces, gray matter thickness was calculated automatically by FreeSurfer at each vertex of the white matter surface for each subject. We computed the mean thickness over the entire cortex for all vertices that were assigned valid anatomical labels by FreeSurfer, while the total brain volume of each subject was calculated using the skull-stripped image generated in FreeSurfer. A template-based retinotopic mapping method described by Benson et al.[15,16] was then applied to generate a parcellation of primary visual areas on the cortical surface. The mean cortical thickness of V1 was computed across both hemispheres.

Diffusion MRI was used to identify differences in the integrity of the optic tracts (the nerve bundles between the optic chiasm and the lateral geniculate nucleus [LGN]) and optic radiation (the massive fiber bundles between the LGN and V1) for each subject. Tract integrity was quantified in terms of fractional anisotropy (FA), radial diffusivity (RD), axial diffusivity (AD), and tract volume. The dMRI data from RP and Argus II subjects were pooled from the three repeated scans to generate a dataset with 90 measurements from 30 gradient directions. For consistency with data from the RP and Argus II subjects, only dMRI images acquired at b = 1000 s/mm^2 were used from the HCP dataset, resulting in 75 gradient directions for each HCP subject. The HCP data were further resampled at 2 mm isotropic spatial resolution to match the RP and Argus II

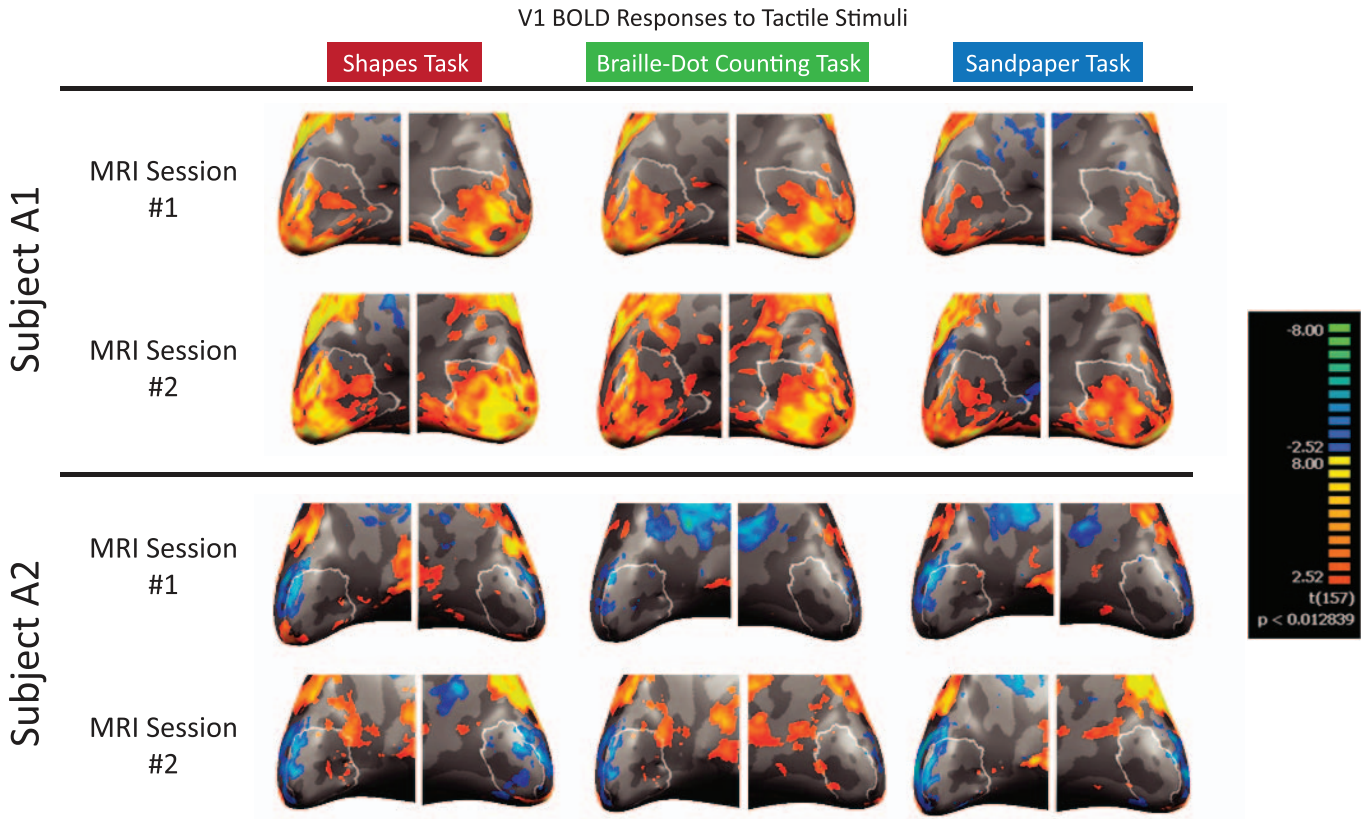

Figure 3. V1 BOLD responses to the three tactile tasks for subjects A1 (*top*) and A2 (*bottom*). Significant responses (FDR < 0.05) were color-coded, with *warm colors* denoting increases in BOLD responses relative to rest. For each subject, the response patterns were projected onto inflated representations of the occipital lobes; the *outer white line* represents the assumed V1/V2 boundary. Right brain hemisphere is on the right.

datasets. After correction for eddy current distortion using FSL,[17] we computed fiber orientation distributions (FODs) with eighth order spherical harmonics using a method described by Tran and Shi.[18] A retinofugal pathway reconstruction method was then applied to the FODs to identify the optic tract and optic radiation fiber bundles.[19] Using a tensor-based analysis, we computed FA, AD, and RD values over the entire image volume. The mean value of each measure was then computed for every fiber bundle to characterize diffusivity. To calculate the volume of each bundle, we first converted the bundle to a tract density image at 1 mm isotropic spatial resolution and then reconstructed a smooth surface representation of the fiber bundle.[20,21] The volume of the bundle was computed as the volume enclosed by the surface. Descriptive statistics were used to compare measurements from the Argus II subjects to those obtained from RP and HCP subjects.

Results

Acquisition of Structural and Functional MR Images in the Presence of the Argus II Implant

A primary concern of MR imaging in Argus II patients was the amount of image distortion that may result from the presence of the implant. For T1w anatomical scans using a 3D MP-RAGE sequence, the implant led to signal drop off and spatial distortion in the vicinity of the implant, including part of the orbitofrontal cortex (Fig. 1, top, red solid arrows). In addition, spatial distortion was also observed extending from the implant along the phase encoding direction (in this case, along the anterior-posterior [AP] axis, Fig. 1, top, orange dashed arrows and ellipse). The nonlocal artifact is mostly related to movement of the eye with the implant and was limited to the hemisphere ipsilateral

to the implanted eye. Its impact can be minimized by having the read-out direction changed to AP, thus limiting the nonlocal artifact to the coronal plane passing through the eyes.

Functional (EPI) images included a similar local artifact in the vicinity of the implant that affected the orbitofrontal cortex of the respective hemisphere (Fig. 1, bottom, solid red arrow). The nonlocal artifact observed with the MP-RAGE acquisition was not apparent in EPI acquisition, consistent with the interpretation that the nonlocal artifact was a result of eye movement, which is slow relative to the duration of slice acquisition with EPI. At no time did the subjects report any unusual sensation that would indicate untoward interaction between the Argus II implant and the scanner and/or applied fields. Fundus exams revealed no observable changes to the implant position. The patients reported that their implants functioned normally after scanning.

DWI scans exhibited a similar local artifact around the implanted eye that affected part of the orbitofrontal cortex (Figs. 2A, 2B; red solid arrows). This artifact did not extend into our ROIs, and no nonlocal noise or distortions were observed, consistent with the fact that the DWI pulse sequence used a single-shot EPI for readout, similar to the functional EPI sequence. Reconstructed retinofugal tracts from both Argus II subjects showed no obvious artifacts when compared to two HCP control subjects (Figs. 2C, 2D).

Tactile-Evoked BOLD Responses in V1 and S1

Neither subject exhibited any responses to the checkerboard stimuli—V1 remained unresponsive to visual stimulation during both MRI sessions with inactive implants.

We measured responses in cortical areas V1 and S1 to each tactile task. The S1 responses to the tactile task, which is intramodal, were strong and extensive as expected (Supplementary Fig. S1; extent [mean ± SD], A1 = [50.7 ± 5.0]%, A2 = [36.7 ± 13.1]%; strength, A1 = 3.5 ± 0.9, A2 = 3.9 ± 0.3]). In contrast, the cross-modal responses in V1 varied between the two subjects (Fig. 3). Subject A1 showed extensive cross-modal V1 responses for all three tasks, while subject A2 did not (extent, A1 = [55.8 ± 11.8]%, A2 = [13.0 ± 6.5]%). Similarly, subject A1 exhibited stronger V1 responses than subject A2 (strength, A1 = 4.0 ± 0.6; A2 = 3.3 ± 0.1).

Comparison of Argus II Subject Responses to Late-Blind RP and Sighted Groups

We further compared the BOLD responses in subjects A1 and A2 to our previous 18 RP and sighted subjects described by Cunningham et al.[10] to determine: (1) if we could effectively measure BOLD signal in the presence of the inactive implant and (2) whether the measurements were comparable to those from subjects without the implant. Based on their visual acuity and visual field, subjects A1 and A2 would belong to the "Blind" category described by Cunningham et al.[10] Subject A1 completed the study 5 weeks after successful implantation of the Argus II device. The extent and strength of her V1 responses to the tactile tasks fell primarily within the range of the blind RP group (Fig. 4). Subject A2 completed our study 15 weeks after successful implantation of the device. In contrast to subject A1, the extent and strength of A2's responses in V1 fell primarily in the range of the low vision RP and normal groups.

We further compared tactile-evoked responses in S1 between the Argus II subjects and RP (blind and low vision) and sighted groups. The extent of subject A1's S1 responses was greater than the 75th percentiles seen across all three subject groups, while the strength of her S1 responses fell within the general variability seen within the blind and low vision groups (Supplementary Fig. S2). A similar comparison found that the extent and strength of subject A2's S1 responses to the tasks were within the ranges of the three groups.

Overall, these comparisons showed that in the presence of the implant, we can obtain good measurements of fMRI BOLD responses that are largely in-line with measurements completed without the implant.

Comparison of Anatomical Measurements Across Argus II, Late-Blind RP, and Sighted Groups

To confirm that the presence of the Argus II implant did not affect acquisition of the structural or DWI data, each Argus II patient's V1 cortical thickness, optic tract, and optic radiation FA, AD, and RD values (across both scanning sessions) were compared to those of the RP and HCP control groups. These measurements from each Argus II patient fell generally within the ranges of the RP and HCP groups (Fig. 5).

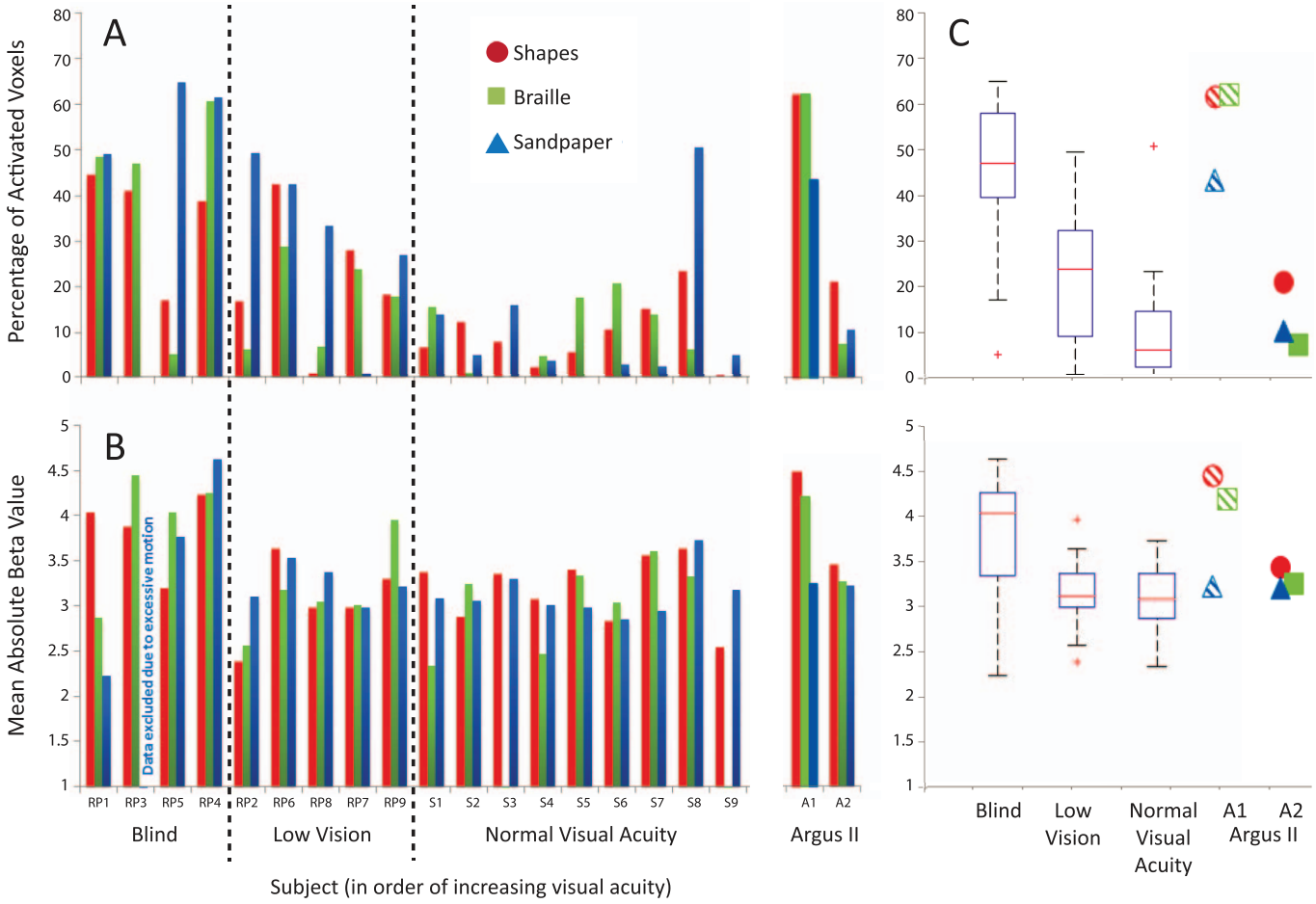

Figure 4. Extent and strength of tactile-evoked cross-modal responses in V1 of Argus II subjects as compared to RP and sighted groups. (**A**) The extent of tactile-evoked fMRI BOLD responses in V1, measured in terms of the percentage of modulated voxels (FDR < 0.05) in V1 for each subject and each task. RP subjects are divided into blind and low vision groups and ranked along the *x*-axis in descending order of severity of visual field loss. (**B**) The strength of tactile-evoked BOLD responses in V1, measured in terms of mean absolute β value of the significantly modulated V1 voxels for each subject and each task. (**C**) Boxplots illustrating the distributions of extent (*upper panel*) and strength (*lower panel*) of tactile-evoked V1 responses in RP (blind and low vision) and sighted control groups across all tasks. The *red line* indicates the mean of each group, the *edges* of the boxes indicate the 25th and 75th percentiles, and the *whiskers* illustrate the most extreme data points. Exact parameter values for each Argus II subject are shown as individual data points for comparison with the RP and sighted control distributions. *Striped shapes*: subject A1. *Solid shapes*: subject A2.

Discussion

The primary concerns in completing MRI scans of Argus II patients, beyond that of patient safety, were the amount and extent of image artifact that would result from the implant. For MP-RAGE, diffusion, and BOLD EPI scans, our data revealed the presence of an artifact that was localized primarily around the patient's implanted eye—this artifact did not extend to other regions of the brain beyond the orbitofrontal cortex immediately adjacent to the implanted eye. In addition, V1 cortical thickness, optic tract, and optic radiation white matter quantifications for the two Argus II patients fell within the ranges of the RP and sighted groups, suggesting these measurements are not grossly affected by the implant. Our results demonstrated that successful data acquisition is possible in retinal implant patients and that normality of the data is maintained.

Results from two Argus II subjects hint at a potential effect of extended use of a retinal prosthesis (and, thus, partial vision restoration), where prosthesis use may decrease tactile-evoked, cross-modal responses in V1. This decrease was evident for subject A2, who had been using the implant for 4 months, but

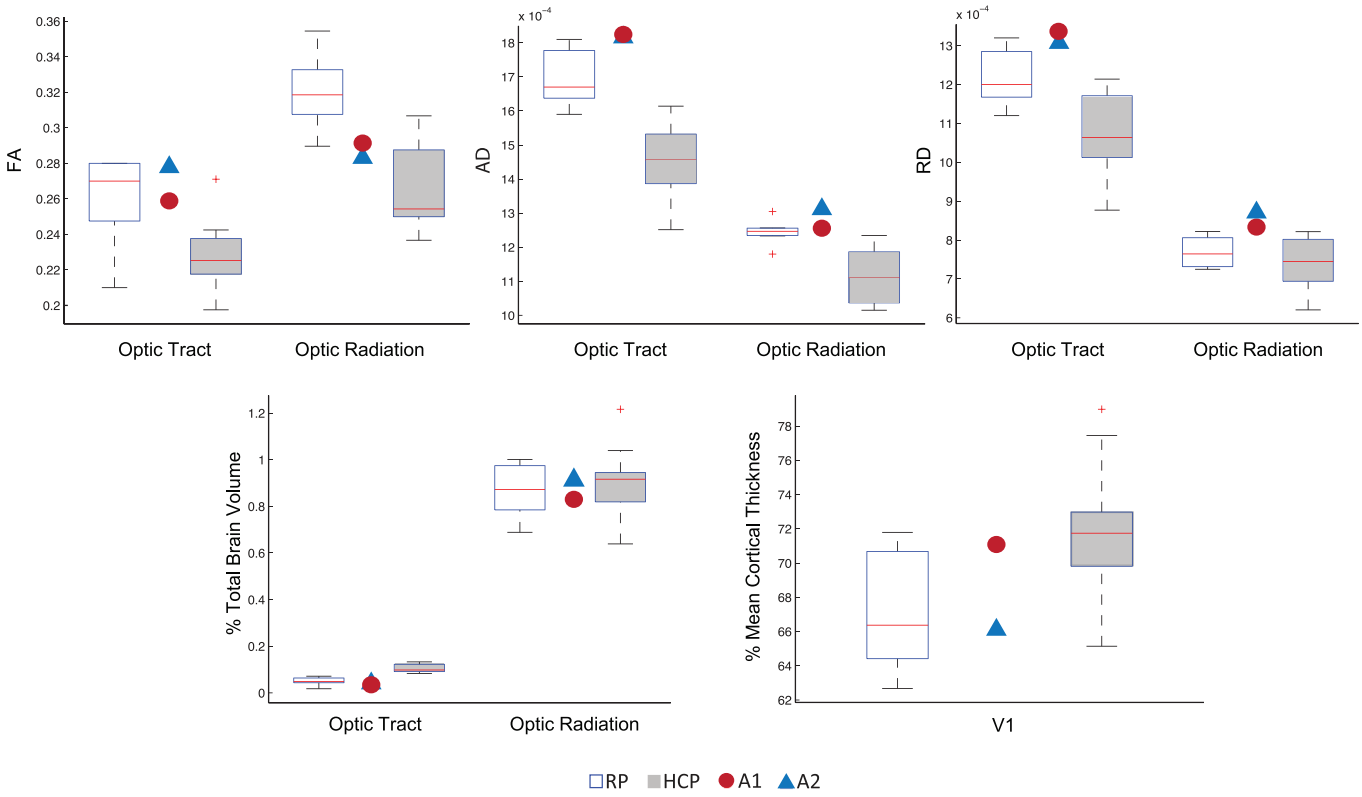

Figure 5. Comparison of structural measurements of the optic tract, optic radiation, and V1 among RP and HCP control subjects with two Argus II subjects. For each subject group, boxplots illustrate the distribution of FA, AD, RD, and normalized volume values for the optic tract and optic radiation. The *red line* indicates the mean of each group, the *edges* of the boxes indicate the 25th and 75th percentiles, and the *whiskers* illustrate the most extreme data points. Exact parameter values for each Argus II subject are shown as individual data points for comparison with the RP and HCP subject groups. V1 cortical thickness values were expressed as a percentage of individual subjects' mean cortical thickness, while tract volumes were expressed as a percentage of individual subjects' total brain volume. AD and RD are in mm^2/s. FA is unit-less.

not A1 after 5 weeks of using the device. Admittedly, data from only two subjects cannot be conclusive, and a larger study population is needed to test this hypothesis.

If a larger cohort of Argus II patients shows that these responses do decrease with extended use of the device, it would mean that cross-modal responses in V1 are gradually suppressed once vision is recovered—the strength and extent of subject A2's responses were reduced compared to other blind RP subjects with a similar visual acuity and visual field. It is also possible that the level of cross-modal activity in V1 may depend on a patient's ability to adapt to the device. That is, cross-modal activity in V1 may be negatively correlated with the visual function regained with the device, where lower levels of cross-modal activity after implantation are associated with greater visual function. It is also conceivable that the presurgery level of cross-modal activity may be related to postsurgery visual function.

Results in two Argus II patients demonstrated the feasibility of acquiring neuroimaging data (anatomical, diffusion, and functional) in the presence of the retinal prosthesis, when the device is in its off state. This provides a basis for further fMRI and MRI studies on the effect of sight restoration treatments on cross-modal responses and structure of visual pathways. Activation of the Argus II in a scanner will require a modified communication coil. If this technical challenge can be overcome, then direct measurement of cortical response appears feasible.

Acknowledgments

Supported by National Science Foundation Grants No. EEC-0310723 and CBET-1353018, National Eye

Institute Grant No. R01EY017707, Research to Prevent Blindness (RPB), the USC Dana and David Dornsife Cognitive Neuroscience Imaging Center, the NSF Graduate Research Fellowship Program (GRFP), National Institute of Biomedical Imaging and Bioengineering Grant No. K01EB013633, P41EB015922, and an unrestricted Departmental grant from Research to Prevent Blindness (New York, NY, USA).

Some results in this study have been reported previously by Cunningham et al.[10] Control data were provided in part by the Human Connectome Project, WU-Minn Consortium (Principal Investigators: David Van Essen and Kamil Ugurbil; 1U54MH091657) funded by the 16 National Institutes of Health (NIH; Bethesda, MD, USA), Institutes and Centers that support the NIH Blueprint for Neuroscience Research; and by the McDonnell Center for Systems Neuroscience at Washington University. The authors alone are responsible for the content and writing of this paper.

Disclosure: **S.I. Cunningham**, None; **Y. Shi**, None; **J.D. Weiland**, None; **P. Falabella**; None; **L.C. Olmos de Koo**, None; **D.N. Zacks**, None; **B.S. Tjan**, None

References

1. Chen Z, Lin F, Wang J, et al. Diffusion tensor magnetic resonance imaging reveals visual pathway damage that correlates with clinical severity in glaucoma. *Clinical Experiment Ophthalmol*. 2013;41:43–49.
2. Li J, Liu Y, Qin W, et al. Age of onset of blindness affects brain anatomical networks constructed using diffusion tensor tractography. *Cerebl Cortex*. 2013;23:542–551.
3. Park H-J, Lee JD, Kim EY, et al. Morphological alterations in the congenital blind based on the analysis of cortical thickness and surface area. *Neuroimage*. 2009;47:98–106.
4. Humayun MS, Dorn JD, da Cruz L, et al. Interim results from the international trial of second sight's visual prosthesis. *Ophthalmology*. 2012;19:779–788.
5. Zrenner E, Bartz-Schmidt KU, Benav H, et al. Subretinal electronic chips allow blind patients to read letters and combine them to words. *Proc Biol Sci*. 2011;278:1489–1497.
6. Raemaekers M, Bergsma DP, van Wezel RJ, et al. Effects of vision restoration training on early visual cortex in patients with cerebral blindness investigated with functional magnetic resonance imaging. *J Neurophysiol*. 2010;105:872–882.
7. Fine I, Wade AR, Brewer AA, et al. Long-term deprivation affects visual perception and cortex. *Nat Neurosci*. 2003;6:915–916.
8. *Argus Retinal Stimulation System Feasibility Protocol*. Available at: http://clinicaltrials.gov/show/NCT00407602.
9. Weiland JD, Faraji B, Greenberg RJ, et al. Assessment of MRI issues for the Argus II retinal prosthesis. *Magn Reson Imaging*. 2012;30:382–389.
10. Cunningham SI, Weiland JD, Bao P, et al. Correlation of vision loss with tactile-evoked V1 responses in retinitis pigmentosa. *Vision Res*. 2015;111(Part B):197–207.
11. Goebel R, Esposito F, Formisano E. Analysis of functional image analysis contest (FIAC) data with BrainVoyager QX: from single-subject to cortically aligned group general linear model analysis and self-organizing group independent component analysis. *Hum Brain Mapp*. 2006;27:392–401.
12. Hinds O, Polimeni JR, Rajendran N, et al. Locating the functional and anatomical boundaries of human primary visual cortex. *Neuroimage*. 2009;46:915–922.
13. Dale AM, Fischl B, Sereno MI. Cortical surface-based analysis. I. Segmentation and surface reconstruction. *Neuroimage*. 1999;9:179–194.
14. Fischl B, Sereno MI, Tootell R, et al. High-resolution intersubject averaging and a coordinate system for the cortical surface. *Hum Brain Mapp*. 1999;8:272–284.
15. Benson NC, Butt OH, Datta R, et al. The retinotopic organization of striate cortex is well predicted by surface topology. *Curr Biol*. 2012;22:2081–2085.
16. Benson NC, Butt OH, Brainard DH, et al. Correction of distortion in flattened representations of the cortical surface allows prediction of V1-V3 functional organization from anatomy. *PLoS Comput Biol*. 2014;10:e1003538.
17. Jenkinson M, Beckmann CF, Behrens TE, et al. FSL. *Neuroimage*. 2012;62:782–790.
18. Tran G, Shi Y. Fiber orientation and compartment parameter estimation from multi-shell diffusion imaging. *IEEE. Trans. Med. Imaging*. 2015;34:2320–2332.
19. Kammen A, Law M, Tjan BS, Toga AW, Shi Y. Automated retinofugal visual pathway recon-

struction with multi-shell HARDI and FOD-based analysis. *Neuroimage*. 2015;123:767–779.
20. Calamante F, Tournier JD, Jackson GD, et al. Track-density imaging (TDI):super-resolution white matter imaging using whole-brain track-density mapping. *Neuroimage*. 2010;53:1233–1243.
21. Shi Y, Lai R, Morra JH, et al. Robust surface reconstruction via Laplace-Beltrami eigen-projection and boundary deformation. *IEEE Trans. Med. Imaging*. 2010;29:2009–2022.
22. Merabet LB, Hamilton R, Schlaug G, et al. Rapid and reversible recruitment of early visual cortex for touch. *PLoS One*. 2008;8:1–12.